Supporting Information

Study of UV-photoexcitation and Ultrafast Dynamics of HCFC-132b (CF_2ClCH_2Cl)

Gessenildo Pereira Rodrigues[1,2*], Elizete Ventura[1], Silmar Andrade do Monte[1], Mario Barbatti[2*]

[1]*Universidade Federal da Paraiba,*

58059-900, Joao Pessoa-PB, Brazil.

[2]*Max-Planck-Institut für Kohlenforschung,*

Kaiser-Wilhelm-Platz 1, 45470 Mülheim an der Ruhr, Germany.

[*] *E-Mail addresses:gessenildo@quimica.ufpb.br (GPR)*

barbatti@kofo.mpg.de (MB)

Figure S1. Graphical representation of the molecular orbitals composing the complete active space (CAS(12,12).

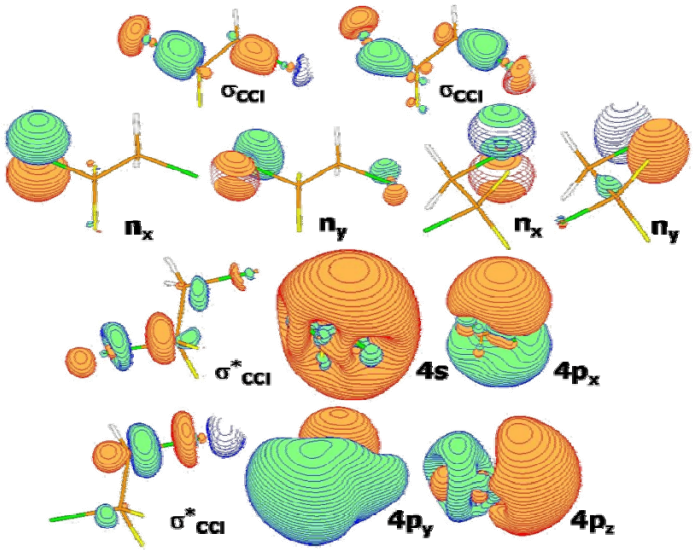

Figure S2. Fitting of the excited-state occupation as a function of time for 8.5 eV (a) and 10 eV (b) excitation windows.

(a)

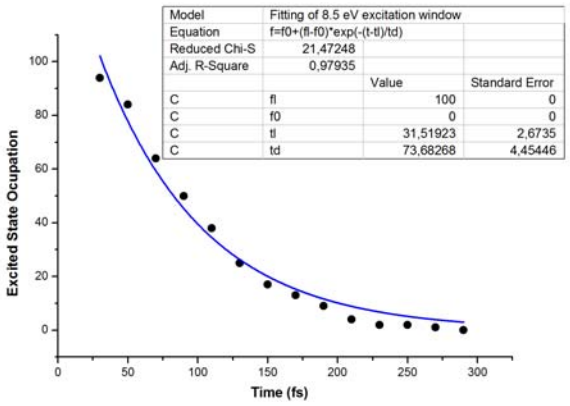

(b)

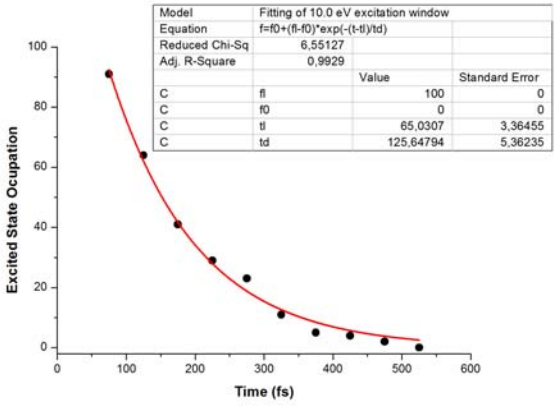

S3. Cartesian Coordinates

Ground state of HCFC-132b. The geometry is in standard XYZ format in Angstrom.

```
C         0.032504    0.486085    0.000000
C        -0.519714   -0.921613    0.000000
Cl       -1.323952    1.630556    0.000000
Cl        0.790714   -2.111749    0.000000
F         0.790714    0.717639    1.082645
F         0.790714    0.717639   -1.082645
H        -1.122280   -1.062027   -0.891737
H        -1.122280   -1.062027    0.891737
```

S4. Vertical-excitation energies (eV), oscillator strengths, and configuration weights obtained for CF_2ClCH_2Cl molecule at the TD-CAM-B3LYP and TD-M062X levels with the aug-cc-pVDZ (C, F, H)/d-aug-cc-pVDZ (Cl) basis set.

States	TD-CAM-B3LYP			TD-M062X		
	ΔE	Weights	f x 10^2	ΔE	Weights	f x 10^2
Gs	0.00	-	-	0.00	-	-
$n_{yCl(3)}$-$\sigma^*_{CCl(3)}$	7.25	0.57	745.90	7.13	0.54	0.14
$n_{xCl(3)}$-$\sigma^*_{CCl(3)}$	7.35	0.58	753.70	7.24	0.55	1.51
$n_{yCl(3)}$-$4p_z$	7.67	0.56	752.90	7.58	0.47	0.89
$n_{yCl(4)}$-$4p_z$	7.68	0.55	759.00	7.60	0.49	0.01
$n_{xCl(4)}$-$\sigma^*_{CCl(3)}$	8.04	0.64	819.80	8.02	0.65	1.18
$n_{yCl(4)}$-$\sigma^*_{CCl(3)}$	8.18	0.64	820.80	8.14	0.65	1.53
$n_{yCl(4)}$-$\sigma^*_{CCl(4)}$	8.85	0.54	906.90	8.82	0.57	7.87
$n_{xCl(3)}$-$4p_z$	8.86	0.54	919.50	8.85	0.59	1.58
$n_{yCl(3)}$-4s	8.91	0.55	921.00	8.92	0.64	1.01
$n_{xCl(3)}$-4s	8.93	0.50	938.00	8.98	0.60	0.19
$n_{xCl(4)}$-$\sigma^*_{CCl(4)}$	9.00	0.63	941.40	9.00	0.50	4.07
$n_{yCl(3)}$-$4p_z$	9.10	0.66	968.70	9.00	0.52	7.77
$n_{xCl(3)}$-$4p_y$	9.55	0.54	979.30	9.39	0.51	0.13
$n_{yCl(4)}$-$4p_x$	9.58	0.38	990.80	9.46	0.34	0.33
$n_{xCl(4)}$-$4p_x$	9.65	0.43	991.50	9.51	0.39	2.39
$n_{yCl(3)}$-$4p_x$	9.69	0.50	998.10	9.56	0.45	7.06
$n_{yCl(4)}$-4s	9.71	0.50	1003.50	9.75	0.62	0.00
$n_{xCl(4)}$-$4p_y$	9.81	0.32	1008.60	9.77	0.43	17.70
$n_{yCl(3)}$-$\sigma^*_{CCl(4)}$	9.82	0.46	1026.80	9.78	0.41	0.11
$n_{yCl(4)}$-$4p_y$	9.88	0.64	1035.40	9.85	0.42	0.72
$n_{xCl(4)}$-4s	9.94	0.57	1043.70	9.90	0.42	0.68
$n_{yCl(3)}$-$4p_y$	10.03	0.55	1044.30	9.91	0.44	1.49
$n_{xCl(3)}$-$\sigma^*_{CCl(4)}$	10.04	0.46	1058.50	10.00	0.37	5.19
$n_{xCl(3)}$-$4p_x$	10.11	0.60	1064.00	10.02	0.49	0.26

Figure **S5**. Comparison between the potential energy curves along the C-Cl bonds, obtained at the CASPT2 and TD-ωB97XD levels.